Determination of Defect States in Semiconductor Nanocrystals by Cyclic Voltammetry

Erol Kuçur,[†] Wendelin Bücking,[†] Ralf Giernoth,[‡] and Thomas Nann*[,†]

Material Research Center, University of Freiburg, Stefan-Meier Straβe 21, 79104 Freiburg, Germany, and Institute of Organic Chemistry, University of Cologne, Greinstraβe 4, 50939 Cologne, Germany

Received: July 15, 2005; In Final Form: August 22, 2005

Colloidal, monodisperse CdSe nanocrystals were homogeneously dispersed in an ionic liquid and investigated by means of cyclic voltammetry. Almost all known defect states in semiconductor nanocrystal were quantitatively measured with this nonoptical method (including nonradiative defect states). Variation of the illumination and temperature resulted in excitation of defect-trapped electrons into the conducting band. Thus, we succeeded for the first time to correlate defect states in nanocrystals with those in the corresponding bulk crystals.

I. Introduction

Although the assumption of a perfectly crystallographically ordered semiconductor crystal with the absence of impurities is sufficient to develop a simplified model for describing a semiconductors' behavior theoretically,[1−4] this assumption is not appropriate for an investigation of the behavior and physical properties of semiconductors, especially CdSe nanocrystals. Every semiconductor bulk material possesses defect states that originate from impurities, divacancies, or surface reactions. At certain critical concentration levels of defects, these materials are adversely affected. Therefore, the effect of the surface reactions of bulk CdSe were investigated thoroughly by the means of surface photovoltage and energy loss spectroscopy by L. J. Brillson[5,6] and other groups.[7−9] Because of the nanocrystals' small number of atoms and their small dimensions, the ratio between the defect states and the nanocrystals net amount of atoms is high compared to their corresponding bulk materials. Thus, the physical properties of these nanomaterials, such as luminescence, are more significantly affected by defects than their bulk material counterparts. The efficiency of luminescence can be decreased rapidly by additional transition levels, caused by the aforementioned defect states in the forbidden band of the semiconductor.

Previous work by Poznyak et al.[10] investigates the band edge as defect states positions of CdTe relative to the vacuum level by means of cyclic voltammetry (CV). Ogawa et al.[11] and Greene et al.[12] previously investigated the charge transport, e.g., the behavior of nanoparticles in CVs under additional light irradiation. This work, therefore, includes the determination of the surface defect states' energy levels in the band gap of CdSe nanocrystals and the investigation of their behavior under excited conditions due to blue-light irradiation.

II. Experimental Methods

A. Chemicals. The chemicals were used as received. The chemicals for the nanocrystal synthesis were: cadmium stearate (Strem chemicals), trioctylphosphineoxide (TOPO, Avacado), selenium (Merck) and trioctylphosphine (TOP, Avocado). Chemicals for the phase transfer of the CdSe quantum dots from chloroform to the ionic liquid: tetradecyltrimethylammonium-bromide (TDTMABr), chloroform, and methanol (Sigma-Aldrich). The ionic liquid 1-dodecyl-3-methylimidazolium-bis-(trifluoromethylsulfonamide) [C_{12} mim][Tf_2N] was synthesized by the group of Ralf Giernoth[13] and dried at 353 K under high vacuum overnight before use.

B. Preparation of Quantum Dots. For a typical preparation of CdSe quantum dots (QDs), 224 mg (330 μmol) of cadmium stearate was placed in a Schlenk flask together with 4 g of trioctylphosphineoxide. The mixture was heated to 333 K and degassed several times. Se (235 mg, 3 mmol) was dissolved in 2 mL of trioctylphosphine, and this solution was injected to the cadmium stearate/TOPO solution at 553 K under Schlenk conditions. The mixture was stirred for 30 min at 523 K, obtaining a red dispersion of nanocrystals. The particles were precipitated with 5 mL of methanol, centrifuged, and redissolved in 20 mL of chloroform. Subsequently, they were characterized by UV−vis and photoluminescence spectroscopy.

C. Phase Transfer of the QDs to the Ionic Liquid. The solution of CdSe nanocrystals in chloroform was washed three times to remove the excess TOPO. In detail, 5 mL of the nanocrystal solution was precipitated with 5 mL of methanol and redissolved in 5 mL of chloroform. This process was repeated twice. Subsequently, tetradecyltrimethylammonium-bromide (TDTMABr) was added to 5 mL of a chloroformic solution of 50.5 mg (0.15 mmol) CdSe nanoparticles and stirred overnight. Finally, 1 mL of this solution of nanoparticles and TDTMABr in chloroform was added to 1 mL of [C_{12}mim]-[Tf_2N]. The chloroform was evaporated in high vacuum at 353 K overnight, resulting in homogeneously dispersed nanocrystals.

D. Apparatus. The UV−vis and photoluminescence spectra were recorded on a J&M TIDAS diode-array spectrometer. Additional absorbance spectra were taken with a halogen/deuterium combined light source. A J&M FL3095 monochromator was used as a monochromatic light source.

Cyclic voltammetric measurements were performed within a homemade electrochemical (EC) inert gas cell, which can be temperature stabilized. A HEKA PG 340 potentiostat/galvanostat was used for the measurement of application and the measurement of the voltage or cell current, respectively. A platinum

* Author to whom all correspondence should be addressed. E-mail: thomas.nann@fmf.uni-freiburg.de.
[†] Material Research Center, University of Freiburg.
[‡] Institute of Organic Chemistry, University of Cologne.

10.1021/jp053891b CCC: $30.25
Published on Web 10/07/2005

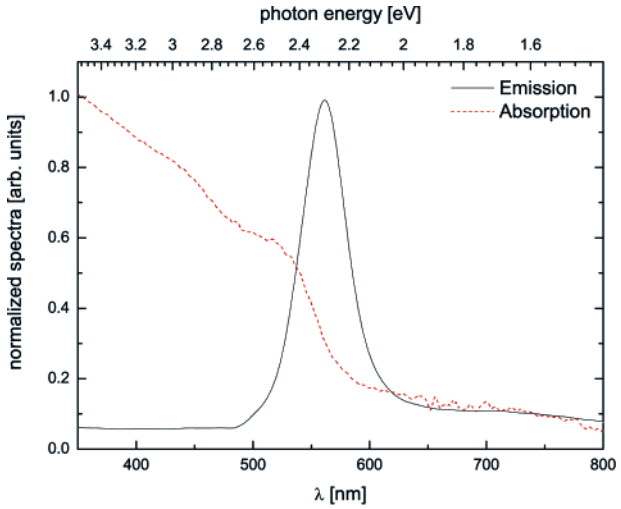

Figure 1. Normalized emission (solid line) and absorption spectra (dashed line) of CdSe/TOPO nanoparticle in chloroformic solution.

electrode of 7.1 mm^2 was used as a working electrode, a platinum wire as a counterelectrode. The reference electrode was built up by a silver wire. Excitation of the nanocrystals was performed during the CV measurement using a blue LED built into the EC cell with an emission wavelength of 470 nm.

III. Results

In addition to the successful measurement of the quantum size effect in CdSe nanocrystals by the means of cyclic voltammetry in one of our previous publications,[14] we could observe a second reduction current peak between the barely observable conduction and valence edges in all measured, differently sized nanoparticles. Impurities stemming from our measuring solution, consisting of acetonitrile and 0.1 M tetrabutylammoniumhexafluorophosphate ($TBAPF_6$, Merck), could be excluded because of further investigations of the solution and the reproducibility of the second current peak. Therefore, we conclude that this peak was caused by an additional energy state located in the band gap of the nanocrystal. This energy state is most likely originated by a defect state, such as a vacancy or impurity. Like in most semiconductors, the existence of only one defect state is a strongly simplified assumption of a crystal lattice. The thorough investigation of CdSe crystals by means of surface photovoltage and energy loss spectroscopy by L. J. Brillson[5,6] and other groups[7−9] revealed several defect states. From comparison, our measured defect state corresponds to one of the defect states measured in the latter publications.[14] The emerging question of why we could not measure the other defect states can be answered by considering the fact that a thin film of nanocrystals was measured in a low conducting media. Thus, we successfully dissolved the nanocrystals in an ionic liquid to provide a measurement setup with increased sensitivity to reduction or oxidation of the nanocrystals.[15]

For all of our investigations herein, we used TOPO-capped CdSe nanocrystals with an emission wavelength of 562 nm and full width at half-maximum (fwhm) of 48 nm. The emission and absorption spectra of these particles are depicted in Figure 1. The ionic liquid [C_{12}mim][Tf_2N] shows an emission peak at 350 nm.[15] Because of the irradiation with a 470 nm blue LED, the ionic liquid was not excited and an energy transfer of excitons from the ionic liquid to the nanocrystals could be avoided effectively.

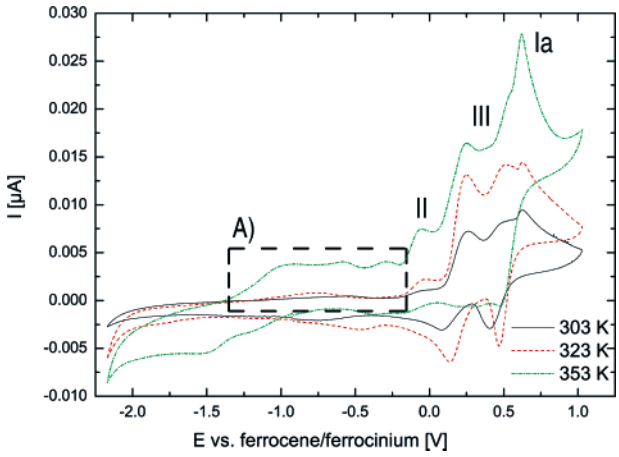

Figure 2. Cyclo voltammogram of CdSe/TOPO nanoparticles in [C_{12}-mim][Tf_2N] at a scan rate of 20 mV/s. The oxidation peak "Ia" refers to the nanoparticles. The labeled region (A) is depicted in Figure 3. The oxidation peaks "III" are caused by TDTMABr.

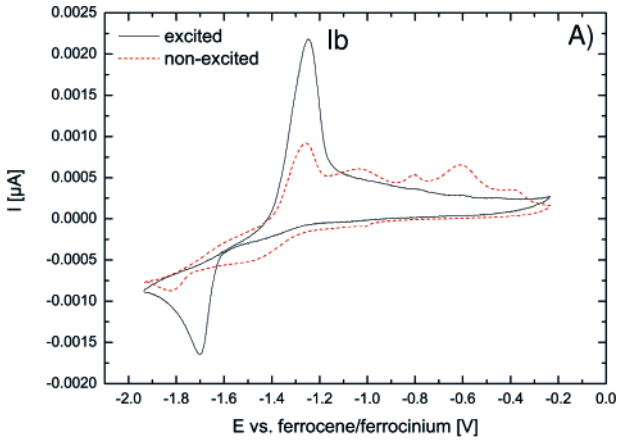

Figure 3. Cyclo voltammogram of CdSe/TOPO nanoparticles in [C_{12}-mim][Tf_2N] at a scan rate of 20 mV/s. The diagram shows the difference of the conduction band ("Ib") current between the excited and nonexcited state at 353 K.

In comparison to recent publications of successfully cyclic voltammetric measured on CdS,[16] PbS,[11] and CdTe[12,10,17] nanocrystals, and to one of our previous publication,[14] the determination of the absolute band edge positions of TOPO-capped CdSe nanocrystals was performed in a more conductive media, namely an ionic liquid, which showed advantages concerning the charge transfer.[15]

A. Cyclic Voltammetric Determination of the Conducting Band of CdSe Nanocrystals. In Figure 2, the temperature-dependent behavior of a cyclic voltammogram of CdSe/TOPO nanoparticles is depicted. It can be clearly seen that the oxidation peaks of the conducting salt (peak "III" in Figure 2) as well as the nanoparticles (peak "Ia" in Figure 2) both increase with temperature. For detailed discussion about the nanoparticles' behavior in ionic liquids, we would like to refer to one of our recently published works.[15] By subtracting the energy value of the oxidation peak ("Ia", 0.6 V), or valence band edge, from the absorption onset potential (2.1 eV), one should observe the conduction band edge in the CV at approximately −1.5 V. As one can see, there is neither a clear reduction nor an oxidation peak for the conduction band under normal illumination. Taking this into account, we cycled the electrode potential in the range where the reduction peak was predicted (cf. Figure 3). To ensure a measurable current peak in this region, we avoided the oxidation of the nanocrystals and, thus, avoided removing

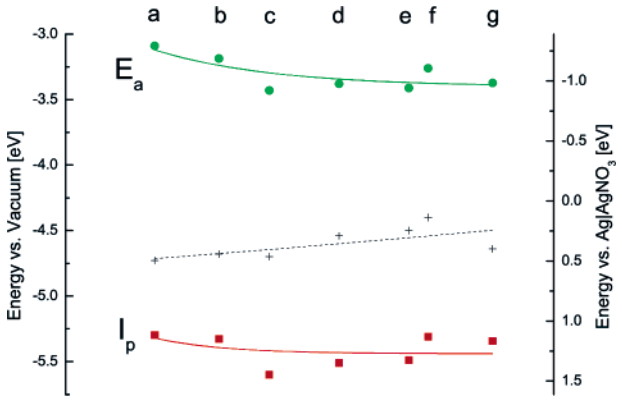

Figure 4. Ionization potential I_P and Electron affinity E_a of different sized nanoparticles (diameters: $a = 2.3$ nm, $b = 3.1$ nm, $c = 3.2$ nm, $d = 3.5$ nm, $e = 3.7$ nm, $f = 3.8$ nm, $g = 4.0$ nm). The values for the E_a were calculated by the addition of the optical band gap to the value of I_P. The data were taken from our previous publications.[14,15]

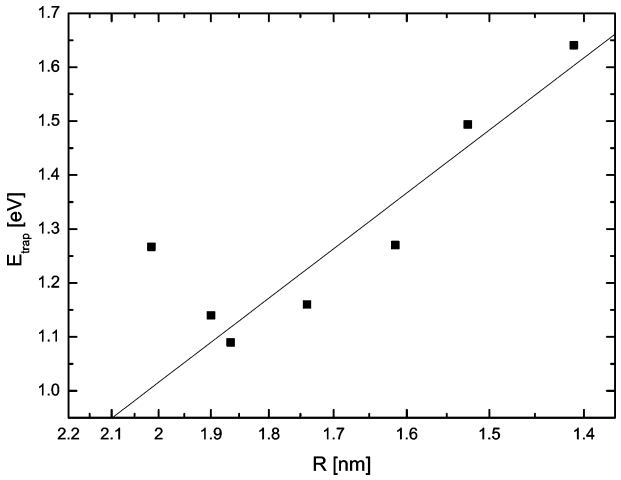

Figure 5. Energy of the deep level defect luminescence E_{trap} from Se/Cd divacancy (cf. (6) in Figure 7) plotted against the corresponding nanoparticles radius R at 303 K. The data were taken from our previous publications.[14,15]

charges from the valence and, subsequently, from the conduction band as it was previously observed.[14] Calculation of the first oxidation peak position of the conduction band using the band gap energy obtained from the absorption spectra and the prominent oxidation peak in Figure 2 shows that the first oxidation peak ("Ib" in Figure 3) at −1.3 V vs ferrocene/ferrocinium can be regarded as the conduction band. We would like to refer to the CV behavior of nanoparticles under blue-light irradiation as additional proof, which is discussed below. The shift of 0.2 V between the predicted and measured value for the conduction band can be explained by a shifted valence as well as a conduction band to lower energy levels due to a lower electron concentration at the surface through the reduction of nanoparticles.

B. Behavior and Origin of Deep States at the CdSe Nanocrystals' Surface. There are several additional oxidation peaks between the valence ("Ia") in Figure 2 and the conduction band ("Ib") in Figure 3, or in the band gap of the CdSe/TOPO nanocrystals. These are either called deep or shallow states depending upon the energy position caused by crystal defects or impurities in the core and impurities on the surface. If one considers the fact that up to 70% of the atoms, depending on the diameter, in such a nanocrystal are surface atoms and the transition from the core to the shell is abrupt (semiconductor−organic material), the presence must be taken into account of at least one defect state. This property could successfully be determined for water-soluble CdTe nanoparticles by Greene et al.[12] In our previous publications,[14,15] we could not only determine the absolute energy levels of the band edges of CdSe nanocrystals, but also defect states in both acetonitrile + 0.1M $TBAPF_6$ and ionic liquid. In all of these measurements, we observed a small oxidation peak next to the current peak caused by the valence band (see peak "II" in Figure 2). Because of the presence of this peak in all differently sized nanocrystals, we could detect a weak linear dependence between the absolute energy position of the peaks and the nanocrystals' diameter (cf. Figure 4). By increasing the nanoparticle diameter or decreasing the ratio between surface and volume atoms, respectively, the energy position of this deep state moves toward lower absolute energy. As predicted and proven by Babentsov et al.[18] and Trojánek et al.[19] a recombination between electrons trapped in shallow traps and holes trapped in deep traps results in a linear dependency of the deep trap energy and the excitonic energy or the radius of the nanoparticles, respectively. To prove whether this defect state is originated by Se/Cd divacancies as it is assumed by deep temperature measurements by Babentsov et al.,[18] we plotted the deep trap energy of differently sized nanoparticles against the radius of these in Figure 5. As one can clearly see, all deep trap energies except the one for the largest studied nanoparticles are in very good agreement with the theory, considering the measurement temperature of 303 K.

The question of why we could not observe any oxidation peak in the band gap in our previous measurement setup with acetonitrile can be answered easily if we consider the electron mobility of the two different conducting media. The ionic liquid has a five times higher conductivity then the acetonitrile system at 303 K and can, therefore, support a more sensitive measurement. This ratio increases up to eight times by increasing the temperature up to 353 K. This also explains the increase of the currents of the oxidation peaks located in the band gap with temperature (cf. dashed window in Figure 2).

Because of the charge mobility, the deep states' current peaks should be affected by an energy supply, such as the increasing temperature or light irradiation. The change in the current peak for the first method can be seen in Figure 2. Here, the deep state peaks are only observable at temperatures higher than 323 K. The result from the latter is depicted in Figure 3. Electrons from these deep states are excited to higher energy levels by blue-light irradiation, resulting in the disappearance of additional oxidation peaks because of the now empty states. As one can easily see, all oxidation peaks disappeared except for the peak related to the conduction band, which increases in total. This can be explained by the fact that the blue light excites all the electrons from the defect states of the band gap to higher allowed energy states, where these electrons move downward to the level of the conduction band by losing energy nonradiatively. The two different processes, namely with and without blue-light irradiation, are depicted in Figure 6.

The question regarding the origin of the defect states arises after the thorough description of the behavior of these defect states. Considering the fact that surface defects are more easily observable by cyclic voltammetry than core defects, some of the measured defect states must be located at the surface of the nanocrystals. In comparison with investigations of the surface structure of CdSe bulk material treated with oxygen,[5−9] our measured values for nanoparticles are in very good agreement with previous measurements (see Table 1). We, therefore, conclude that some surface defects are caused by oxygen adsorption at cadmium surface atoms. The oxygen from the

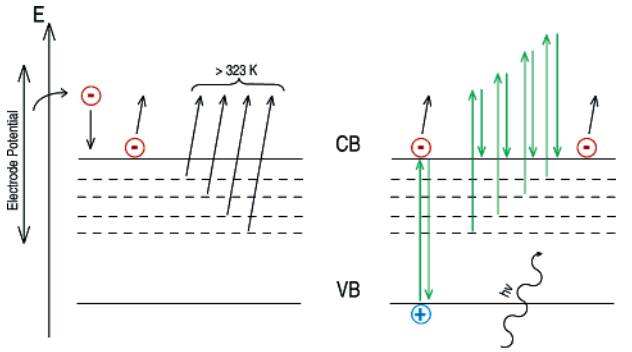

Figure 6. Sketch of the CdSe nanocrystals band edge positions and their deep trap states relative to the edges.

TABLE 1: Comparison between the Absolute Energy Positions of the Defect States below the Conduction Band Obtained by the Cyclic Voltammetry Δ (Left-Hand Side in the Table) with the Data Obtained Through Other Investigations

Δ [eV]	Brillson[a]	Brillson[b]	Hoffmann[c]	Türe[d]	Bube[e]
0.21	0.14	0.16	0.12/0.15	0.13	n.a.
0.45	0.43	0.56	n.a.	n.a.	n.a.
0.64	0.70	n.a.	n.a.	n.a.	0.79
0.91	1.05	1.04	n.a.	1.16	1.05
1.25	1.4	1.36	n.a.	1.36/1.46	1.20

[a] From ref 5. [b] From ref 6. [c] From ref 7. [d] From ref 8. [e] From ref 9.

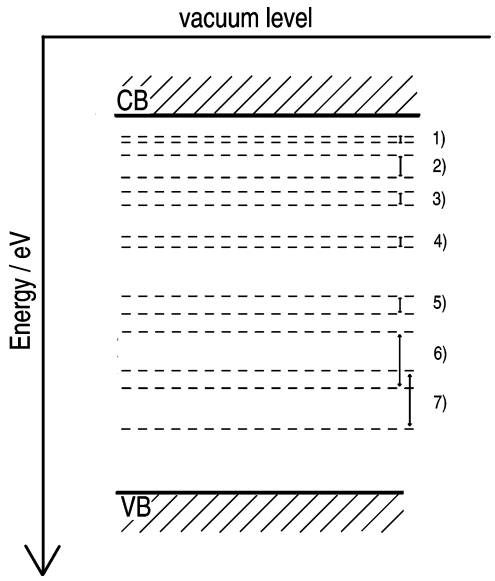

Figure 7. Sketch of the defect states in CdSe nanocrystals relative to the band edges. Defect states originated from (1) and (3): Se divalent vacancies;[20] (2): Se vacancy,[21] (4) and (5): oxygen;[5−9] (6) and (7): Se/Cd divacancies.[18,22] Energy level regions [eV] of defect states relative under the conduction band: (1) 0.11−0.15; (2) 0.21−0.33; (3) 0.4−0.47; (4) 0.64−0.70; (5) 0.95−1.05; (6) 1.15−1.45; (7) 1.35−1.66.

TOPO shell seems to be the most obvious "contamination" origin, but further origins should not be neglected, such as the interface between nanocrystal solution−air and the oxygen contained in the chemicals used. To clarify the origins of the other defect states, we summarized the energy positions of defect states in CdSe material cited in the literature in Figure 7. A comparison of this with our results listed in Table 1 shows that we could successfully measure the defect states of Se (2), Se divalent (3), oxygen vacancies (4 and 5), and Se/Cd divacancy (6). The determination of the second Se/Cd divacancy (7) was not detectable because of the predominant oxidation peak of the ionic liquid.

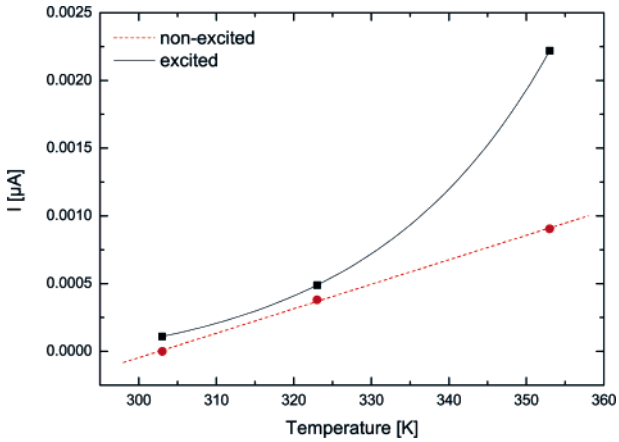

Figure 8. Temperature and irradiation dependency (excited: solid line (square); nonexcited: dashed line (circle)) of the current taken from the oxidation peak of the conduction band "Ib". The linear and exponential fits are guidelines for the eyes.

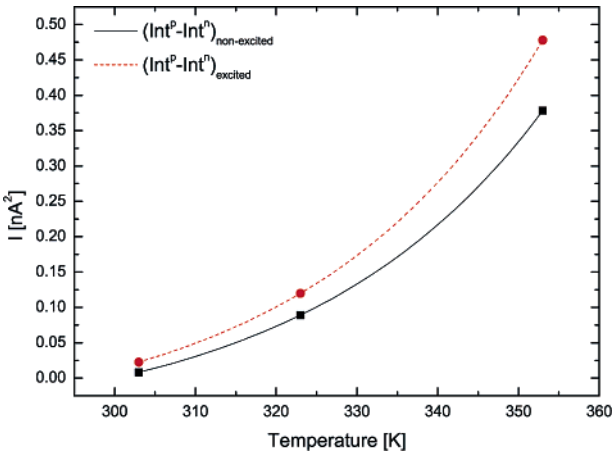

Figure 9. Temperature dependency of the net amount of electrons in both cases excited (solid line (square)) and nonexcited (dashed line (circle)), respectively. The exponential fits are guidelines for the eyes.

Discussion

For a better understanding of how temperature effects the excitation dependency of the charges, the current from the oxidation peak "Ib" was depicted in relationship to the two states, namely, excited (solid curve) and nonexcited (dashed curve), in Figure 8. At relatively low temperatures up to 325 K, the difference between the excited and nonexcited state is approximately a few nanoamperes. By increasing the temperature up to 353 K, this difference increases to a few microamperes. The conductivity change of the ionic liquid with temperature can be seen to be weakly linear (not shown), while the conductivity change in our measurement can be seen to be exponential. We can assume, therefore, that the charges are more mobile at a higher temperature and less mobile at low temperatures, which is in complete agreement with common semiconductor theory. Furthermore, the diffusion coefficient of the nanocrystals increases with increasing temperature as well.

Whereas the aforementioned examination only included the current value of the conduction band, Figure 9 depicts the difference between the oxidation and the reduction area in the excited and nonexcited states, or simply, the graph shows the net amount of electrons (corresponding with the *concentration*

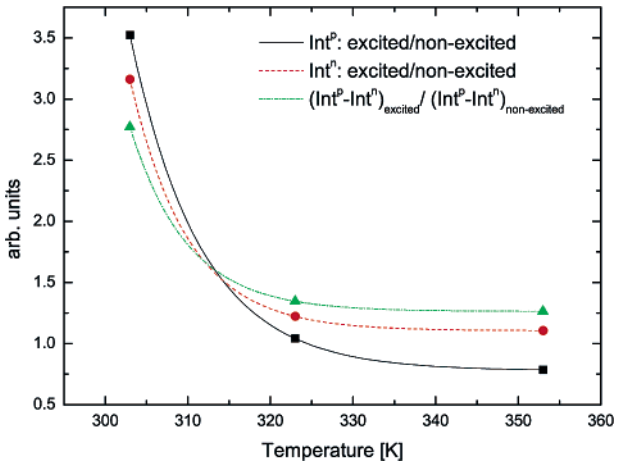

Figure 10. Temperature dependency of ratios between the net amount of forced in ("Int^n") and taken out ("Int^p") electrons as well as the total net amount of electrons in both excited and nonexcited cases. The exponential fits are guidelines for the eyes.

of states!). Here, we distinguish the amount of electrons forced in ("Int^n", dashed line (circles)) and taken from ("Int^p", solid line(squares)) the nanocrystal. As one can easily see, the net electron amount exponentially increases with increasing temperature in both conditions. This effect is caused by the higher mobility of the charges in nanocrystals and the higher conductivity of the ionic liquid. It has to be noted, furthermore, that more electrons contribute to the measurement at higher temperatures because of their higher charge mobility ($m_e = 0.11$ m_0) than holes ($m_h = 0.44$ m_0).

To better differentiate, the ratio of the net amount of electrons forced in and taken from the nanocrystals in each case, namely the excited and nonexcited states, are depicted in Figure 10. At low temperatures, the ratio between the excited and nonexcited states is approximately three times bigger than at high temperatures. The ratio of the amount of electrons added to the nanocrystal in the excited and nonexcited states decreases to nearly equal by increasing temperature ("Int^n"). This behavior lead us to the conclusion that the thermal energy at high temperatures is sufficient to mobilize the electrons in the nanocrystal and the deep states thoroughly. It can be seen that a further exciting of the electrons by irradiation no longer has a strong effect. Another conclusion is that more electrons are removed from the nanocrystals ("Int^p") at low temperature than those added ("Int^n") by irradiation. Yet, this behavior inverses with increasing temperature around 313 K, indicating the stronger predominant influence of the temperature.

An additional interesting fact is that the ratio between the excited and nonexcited electrons removed from the nanocrystals fell below one at high temperatures. This behavior can be explained by considering the charges generated by the blue-light irradiation. We infer that the electrons irradiated by the blue light at high temperatures recombine with the generated holes in the valence band radiatively, just as it was already proven for different nanocrystals such as CdTe, CdSe, CdSe/ZnSe, and CdSe/CdS.[17,23−25] We assume that this effect, although less strong, also occurs at low temperatures. Therefore, taking into account the cell current behavior depicted in Figure 8, this effect predominates at high temperatures.

For further understanding of the nanocrystals' behavior in ionic liquids, the ratio between the net amount of electrons in the excited and nonexcited state is depicted as the dash−dotted line (triangles) in Figure 10. As one can easily see, this behavior follows an exponential decay dependent on the temperature. At low temperatures, it is possible to add more electrons in the conduction band from the valence band, or deep states than at relatively high temperatures. This supports the above-mentioned assumption of recombinations of the charges occurring at high temperatures and the higher conductivity of the ionic liquid. Further increasing the temperature above 353 K reveals only small changes in the ratio between the net amount of electrons in the excited and nonexcited state.

V. Conclusions

We were able to measure defect states of nanocrystals by the means of cyclic voltammetry due to a more conductive media, here, an ionic liquid. The absolute energy position behavior of one of these could be investigated by the variation of the nanocrystal size, along with the quantum-size dependency of the band edges. We could further prove that this defect state is originated by a recombination of electrons and holes trapped in shallow and deep traps, respectively. In addition, the effect of the change of temperature as well as the effect of blue-light irradiation on the behavior of electrons capped in these states, was successfully investigated.

Because of the good agreement of our results with the results obtained by surface photovoltage and energy loss spectroscopy, cyclic voltammetry can be considered as an effective measurement technique for the determination of defect states in the forbidden band.

Acknowledgment. We acknowledge the help of Britta Rotzinger for preparation of the QDs and Sven Arenz for the preparation of the ionic liquids. Additionally, they thank Pamela Z. Espindola for her support with conductivity measurements of ionic liquids. E.K. and W.B. thank the state of Baden-Württemberg and the Federal Ministry of Education and Research (BMBF) for financial support within the projects AZ 24-720.431-1-7/2 and FKZ 13N8644.

References and Notes

(1) Brus, L. E. *J. Chem. Phys.* **1983**, *79*, 5566−5571.
(2) Norris, D. J.; Efros, A. L.; Rosen, M.; Bawendi, M. G. *Phys. Rev. B* **1996**, *53*, 16347−16354.
(3) Poles, E.; Selmarten, D. C.; Mićić, O. I.; Nozik, A. J. *Appl. Phys. Lett.* **1999**, *75*, 971−973.
(4) Sapra, S.; Sarma, D. D. *Phys. Rev. B* **2004**, *69*, 125304-1−125304-7.
(5) Brillson, L. J. *J. Vac. Sci. Technol.* **1975**, *13*, 325−328.
(6) Brillson, L. J. *Surf. Sci.* **1977**, *69*, 62−84.
(7) Hoffmann, H. J.; Huber, E. *Physica B & C* **1981**, *111*, 249−256.
(8) Türe, I. E.; Russell, G. J.; Woods, J. *J. Cryst. Growth* **1982**, *59*, 223−228.
(9) Bube, R. H. *Phys. Rev.* **1955**, *99*, 1105−1116.
(10) Poznyak, S. K.; Osipovich, N. P.; Shavel, A.; Talapin, D. V.; Gao, M.; Eychmüller, A.; Gaponik, N. *J. Phys. Chem. B* **2005**, *109*, 1094−1100.
(11) Ogawa, S.; Hu, K.; Fan, F.-R. F.; Bard, A. J. *J. Phys. Chem. B* **1997**, *101*, 5707−5711.
(12) Greene, I. A.; Wu, F.; Zhang, J. Z.; Chen, S. *J. Phys. Chem. B* **2003**, *107*, 5733−5739.
(13) Giernoth, R.; Krumm, M. *Adv. Synth. Catal.* **2004**, *346*, 989−992.
(14) Kucur, E.; Riegler, J.; Urban, G. A.; Nann, T. *J. Chem. Phys.* **2003**, *119*, 2333−2337.
(15) Kucur, E.; Bücking, W.; Arenz, S.; Giernoth, R.; Nann, T. *Chem. Phys. Chem.* **2005**, in press.
(16) Haram, S. K.; Quinn, B. M.; Bard, A. J. *J. Am. Chem. Soc.* **2001**, *123*, 8860−8861.
(17) Bae, Y.; Myung, N.; Bard, A. J. *Nano Lett.* **2004**, *4*, 1153−1161.
(18) Babentsov, V.; Riegler, J.; Schneider, J.; Ehlert, O.; Nann, T.; Fiederle, M. *J. Cryst. Growth* **2005**, *280*, 502−508.
(19) Trojanek, F.; Cingolani, R.; Cannoletta, D.; Mikes, D.; Nemec, P.; Uhlirová, E.; Rohovec, J.; Maly, P. *J. Cryst. Growth* **2000**, *209*, 695−700.
(20) Skarman, J. S. *Solid-State Electron.* **1965**, *8*, 17−29.
(21) Lee, S.-C.; Lee, M. J. *J. Appl. Phys.* **2000**, *88*, 1999−2001.
(22) Blachnik, R., Chu, J., Galazka, R. R., Geurts, J., Gutowski, J., Hönerlánge, B., Hoffmann, D., Kossut, J., Levy, R., Michler, P., Neukirch,

U., Story, T., Strauch, D., Waag, A., Eds. *II−VI and I−VII Compounds, Semimagnetic Compounds*; Springer-Verlag: New York, 1999; Vol. 41B.
(23) Myung, N.; Ding, Z.; Bard, A. J. *Nano Lett.* **2002**, *2*, 1315−1319.
(24) Myung, N.; Bae, Y.; Bard, A. J. *Nano Lett.* **2003**, *3*, 1053−1055.
(25) Poznyak, S. K.; Talapin, D. V.; Shevchenko, E. V.; Weller, H. *Nano Lett.* **2004**, *4*, 693−698.